

In situ FT-IR spectroscopy study on the conformational changes of quenched isotactic polypropylene during stepwise heating

Junchai Zhao · Zheng Peng · Jianmin Zhang · Gengchen Li

Received: 1 September 2010 / Revised: 13 June 2011 / Accepted: 15 June 2011 /
Published online: 22 June 2011
© Springer-Verlag 2011

Abstract The conformational changes of quenched isotactic polypropylene (iPP) during stepwise heating have been carefully studied by in situ Fourier-transform infrared (FT-IR) spectroscopy. Analysis of the corresponding spectra shows that the mechanism of the extension of short helix into long one happens. Furthermore, it is easier for short helix at 998 cm^{-1} band to extend into long one than that of short helix at 973 cm^{-1} band. Meanwhile, for the higher order regularity band at 841 cm^{-1} , the melting-recrystallization seems to occur. However, the number of the higher order regularity band at 1220 cm^{-1} hardly remains change, which shows the limited increment of the higher order regularity band for quenched iPP in the whole heating process. In summary, two proposed mechanisms, the extension of short helix into long one and the melting-recrystallization of the long helix, happen during stepwise heating, which may give us new insights on the mesomorphic-to-monoclinic phase transition mechanism of quenched iPP from a molecular structure viewpoint.

Keywords Conformational changes · FT-IR · Isotactic polypropylene

Introduction

It is well known that for iPP, besides α , β , and γ , the three crystallization modifications, there is also a mesomorphic phase which can be obtained by rapid quenching from the melt [1–3]. A tentative classification of mesophases was reported by Wunderlich [4], who divided mesophases into six different types of phases: liquid crystals (LC), condensation crystals (CD), plastic crystals (PC), and the corresponding LC,

J. Zhao (✉) · Z. Peng · J. Zhang · G. Li
School of Material Science and Engineering, Shijiazhuang Tiedao University,
Shijiazhuang 050043, People's Republic of China
e-mail: f-angle@163.com

CD, and PC glasses. Note that all these mesophases show large-amplitude motion in addition to the always present small amplitude, vibrational motion. According to Wunderlich [4], CDs consist of flexible molecules which can easily undergo changes in the conformation without losing positional or orientational order [4]. And conformationally disordered or CD glasses are obtained by quenching CDs below their glass transition temperature. Therefore, as discussed in [4], in a CD cooperative motion between various conformational isomers is permitted, whereas in the CD glass this motion is frozen, but the conformationally disordered structure remains. By 1984, the mesophase of iPP was identified as a CD glass [5].

Up to now, the structure of quenched iPP is still not fully resolved. Initially, four types of structure of the quenched iPP have been proposed [6], i.e., “smectic form” [1], “paracrystal” [7], “small hexagonal crystals” [8], and “micro monoclinic crystals” [9]. On the basis of X-ray diffraction patterns and IR spectra it was recognized [1, 2] that mesomorphic phase is organized in a state intermediate between the crystalline and amorphous phases. It contains parallel helices of different handedness [2], with the same 3_1 helix as seen in the crystalline polymorphs. Moreover, the packing is less dense and the unit cell parameters in inter-helical direction are increased in the mesomorphic structure. The literature suggests helix reversals as major reason for the increased inter-chain packing, i.e., a random occurrence of left-handed and right-handed helices [1, 2]. Later, it was confirmed that the mesophase contains bundles of parallel aligned chains with a 3_1 helical conformation, but being terminated in direction of the chain axis by helix reversals or other conformational defects [10]. However, these structure suggestions did not consider the conformational motion, which would produce an average structure of short chain length segments not resolved by the X-ray analysis, as mentioned in literature [11].

Because mesomorphic phase has important implications, it can be considered as a precursor for generation of a specific semi-crystalline structure with a combination of optical and mechanical properties which is qualitatively different from that of conventionally crystallized material [12]. In recent years, there is still of interest in studying mesomorphic phase, including the influence of molecular parameters on the formation of mesophase [13], mechanical behavior [14], thermodynamic stability [15], morphology [16, 17], phase transition mechanism [18–21], and evolution of quenched structure with temperature [22].

Among these researches, the mesomorphic-to-monoclinic phase transition mechanism for initially quenched iPP was widely investigated by small-angle X-ray scattering/wide-angle X-ray diffraction (SAXS/WAXD) [18, 20] and atomic force microscopy (AFM) [16, 19], respectively. Wang et al. [18] proposed that the mesomorphic-to-monoclinic phase transition follows a sequence that begins with a partial melting process, which leaves intact the local lateral ordering of the chains while allowing a correct registration of their helical hands, and is followed by a secondary nucleation that transforms mesomorphic nodules into lamellae. However, by using in situ AFM, Androsch [19] observed the crystal morphology as a function of temperature to further track the mechanism of the mesomorphic-to-monoclinic phase transition and found that initially mesomorphic domains were not destroyed during the phase transformation but could not rule out local melting within domains.

Consequently, it is unclear if the mesomorphic-to-monoclinic phase transition occurs via melting into the liquid state or rather by a direct solid-to-solid transition. Two potential mechanisms, reversing helix handedness and chain motion (translation) while retaining handedness, have been provided to explain the mesomorphic-to-monoclinic phase transition. Recently, Marega et al. [20] reported that mesomorphic-to-monoclinic phase transition of quenched iPP involves in a rearrangement of the chains without a melting-recrystallization process according to the results of SAXS/WAXD.

It is evident that the phase transition mechanisms proposed above for quenched iPP are controversial. No doubt, the exact mechanism of the mesomorphic-to-monoclinic phase transition on heating is not well-explored yet. So, it is quite necessary to trace the temperature-induced changes of structure of initially quenched mesomorphic iPP by in situ FT-IR to reveal the phase transition mechanism at the level of molecular segments. In this study, the conformational changes of quenched mesomorphic iPP during stepwise heating have been concerned. It is expected to give us new insights on the mesomorphic-to-monoclinic phase transition mechanism of initially quenched iPP from a molecular structure viewpoint.

Experimental

Materials and sample preparation

An iPP sample, with number and weight-averaged molecular masses, M_n and M_w , of 97,000 and 340,000, respectively, bought from the Aldrich Chemical Company was used in this study. The isotacticity index of the iPP obtained by *n*-heptane extraction is about 0.976. The iPP film with thickness of about 20 μm sandwiched between two silicon wafers was heated to 200 $^\circ\text{C}$ and held for 15 min, and then was quickly immersed into liquid nitrogen to prepare mesomorphic film.

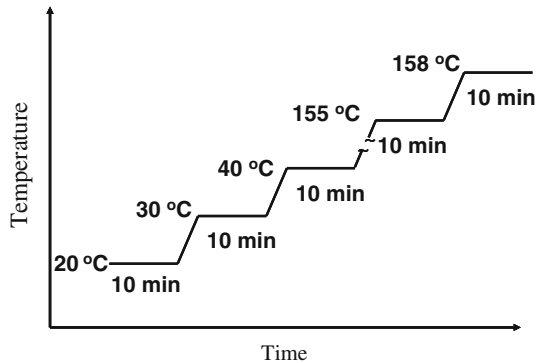
Wide-angle X-ray diffraction (WAXD) measurements

The WAXD measurements on the iPP film samples used for FT-IR characterization were carried out by using a Bruker D8 Discover diffractometer equipped with GADDS as the two-dimensional (2D) detector. Samples were mounted on the sample stage and the point-focused X-ray beam was aligned perpendicular to the sample plane. 2D WAXD patterns were recorded at room temperature in transmission geometry, from which the WAXD profiles of the isotropic patterns were extracted by azimuthal averaging.

FT-IR measurements

The time-resolved FT-IR measurements were performed on a Bruker Tensor27 FT-IR spectrometer equipped with a variable temperature cell. The temperature was raised stepwise, holding 10 min at each temperature before the measurement (Fig. 1). The measurements were conducted at 20, 30, 40, 60, 80, 90, 100, 110, 120,

Fig. 1 Temperature protocol for the FT-IR measurements



130, 140, 150, 155, and 158 °C, respectively. Here, the intensity refers to peak height. To different peak shape, a suitable method for calculating the peak height and drawing the baseline was chosen from the Bruker OPUS software. The resolution is 4 cm^{-1} , and the scanned wavenumber ranges from $4000\text{ to }400\text{ cm}^{-1}$.

Results and discussion

Figure 2 displays the WAXD profile of quenched iPP film at room temperature. It is clear that mesomorphic phase is generated indeed when the molten iPP film was quenched into liquid nitrogen. Two broad peaks at around $2\theta = 15^\circ$ and 21° can be observed, which are known as characteristic features of mesomorphic phase of iPP. It is recognized that the first broad peak is related to the average distance between parallel aligned chains in the mesophase and the second one to the repeating period within the 3_1 helix of an isotactic sequence of the macromolecule [1, 6, 15].

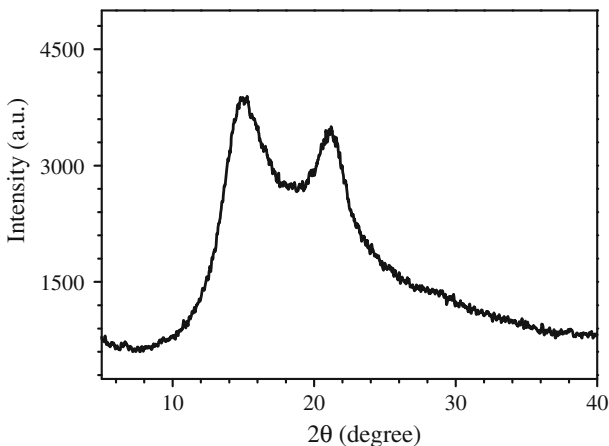


Fig. 2 WAXD profile of quenched iPP film at room temperature

It has been well established that the regularity bands of a polymer originate from the intramolecular coupling oscillations of the various atomic groups [23]. In FT-IR spectra, the major proportion of the iPP molecules are in a 3_1 helical conformation and the bands of 1330, 1303, 1220, 1167, 1100, 998, 940, 900, 841, and 808 cm^{-1} all belong to the regularity bands or helix bands. These bands are related to the different helical lengths of isotactic sequences [24]. The minimum sequence length (n) of isotactic monomer units being sufficient for the appearance of the 973, 998, 841, and 1220 cm^{-1} bands is 3–4, 10, 12, and 14 or more helical units, respectively [25–27]. Apparently, the larger the value of n , the higher the degree of order of the correspondent regularity bands. In quenched iPP, the chains show a 3_1 helical conformation, which is just the same as the α -monoclinic crystal of iPP [7].

The infrared spectra of quenched iPP recorded during stepwise heating are shown in Fig. 3. The band assignments marked in Fig. 3 are used for the structural analysis. It is clear that the intensities of iPP helix sequence at 973, 998, 841, and 1220 cm^{-1} are enhanced, indicating an increase of content of the relevant regularity band with temperature increasing. That is to say, the intensity increment is in proportion to the content of the regularity bands, which shows an ordering of iPP helix sequences by heating. Since the band at 1460 cm^{-1} results from the asymmetric deformation vibration of the methyl group, it serves as an internal standard [28] to avoid the effect of film thickness of each sample. Figure 4 is the plot of the ratio of intensity for various regularity bands with temperature. From Fig. 4a, it can be seen that with $120\text{ }^\circ\text{C}$ as a boundary, the ratio of band intensities at 973 and 1460 cm^{-1} linearly decreases before $120\text{ }^\circ\text{C}$. While after $120\text{ }^\circ\text{C}$, it basically remains invariable. This fact reveals that a structure change occurs in the vicinity of $120\text{ }^\circ\text{C}$. Furthermore, we can infer that the mechanism of extension of short helix at 973 cm^{-1} into long one is dominant when the temperature is lower than $120\text{ }^\circ\text{C}$. However, the other mechanism of the formation of short helix from amorphous phase cannot be excluded. When the temperature is higher than $120\text{ }^\circ\text{C}$,

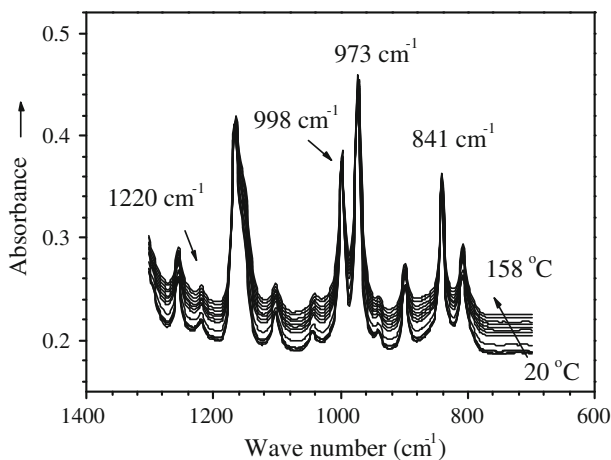


Fig. 3 IR spectra of quenched iPP at annealing temperature of 20, 30, 40, 60, 80, 90, 100, 110, 120, 130, 140, 150, 155, and $158\text{ }^\circ\text{C}$ for 10 min, respectively

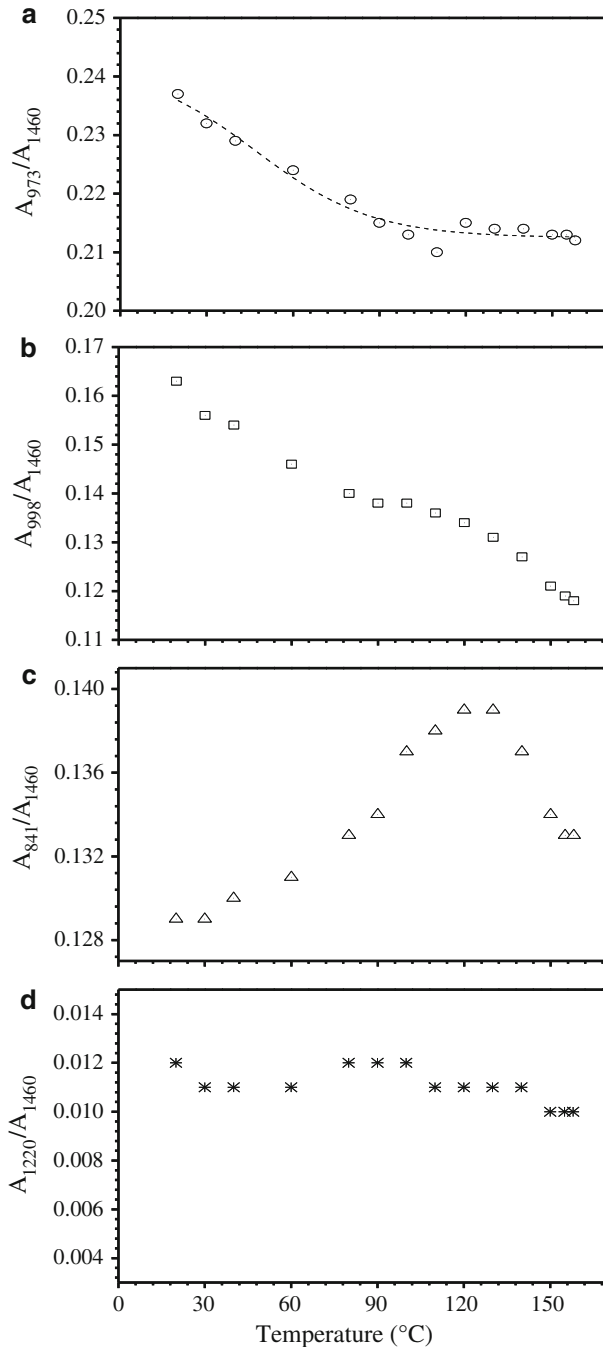


Fig. 4 The plot of intensity ratios of different regularity bands versus temperature from 20 to 158 °C: **a** $A_{973} \text{ cm}^{-1}/A_{1460} \text{ cm}^{-1}$, **b** $A_{998} \text{ cm}^{-1}/A_{1460} \text{ cm}^{-1}$, **c** $A_{841} \text{ cm}^{-1}/A_{1460} \text{ cm}^{-1}$, and **d** $A_{1220} \text{ cm}^{-1}/A_{1460} \text{ cm}^{-1}$

the constant content of the 973 cm^{-1} band gives a clue that probably the two mechanisms, the formation of 973 cm^{-1} band from amorphous phase and the extension of 973 cm^{-1} band into long one, are in equilibrium. For the 998 cm^{-1} band, the ratio of band intensities at 998 and 1460 cm^{-1} decreases almost in linearity, which implies that the extension of helix band at 998 cm^{-1} into long one is dominant in the whole heating process (Fig. 4b). As for the 841 cm^{-1} band, the ratio of band intensities at 841 and 1460 cm^{-1} increases in the first stage then decreases in the second with $120\text{ }^\circ\text{C}$ as a boundary. Therefore, it can be said that when the temperature is lower than $120\text{ }^\circ\text{C}$ two possible factors which lead to the increase of the content of 841 cm^{-1} band can exist. One is the extension of initially short helical segments (such as 973 and 998 cm^{-1}) within the mesophase. The other is the ordering of initially amorphous segments. While when the temperature increases to $120\text{ }^\circ\text{C}$ or even higher, the content of the 841 cm^{-1} band decreases likely due to the occurrence of melting-recrystallization (Fig. 4c). Previous literatures [16, 29, 31] also reported that the increasing nodular size, the slight variation of the aspect ratio of nodule, and even a change of nodular geometry for quenched mesomorphic iPP were observed when the annealing temperature is higher than $120\text{ }^\circ\text{C}$, all of which are considered relating to the melting-recrystallization of initial nodular domains. So, it can be said that the melting-recrystallization probably exists indeed when the annealing temperature is higher than $120\text{ }^\circ\text{C}$ for quenched mesomorphic iPP. The ratio of band intensities at 1220 and 1460 cm^{-1} has almost no variation on the whole during stepwise heating, meaning that no detectable extension of shorter helix (such as 973 and 998 cm^{-1}) into 1220 cm^{-1} happens in the whole heating process (Fig. 4d).

To obtain further information about heat-induced conformational changes, the relative variations of the regularity bands at 973 , 998 , 841 , and 1220 cm^{-1} are investigated. Figure 5 presents the evolution of the ratios of different helix sequences with temperature. For the longest regularity band at 1220 cm^{-1} and the shortest regularity band at 973 cm^{-1} (shown in Fig. 5a), it can be considered that the ratio of band intensities at 1220 and 973 cm^{-1} has no evident variation on the whole during stepwise heating. That is to say, no detectable extension of short helix at 973 cm^{-1} into 1220 cm^{-1} appears during heating, which implies that the content of higher order regularity band at 1220 cm^{-1} cannot be increased at the expense of extension of short helix by stepwise heating. The relative change of regularity bands at 841 and 973 cm^{-1} during stepwise heating is shown in Fig. 5b. Obviously, when the temperature is lower than $120\text{ }^\circ\text{C}$, the ratio of band intensities at 841 and 973 cm^{-1} increases, indicating a significant growth of long helix chains at 841 cm^{-1} due to the extension of short helix at 973 cm^{-1} . But when the temperature is higher than $120\text{ }^\circ\text{C}$, the ratio drops, illustrating that perhaps the content of the regularity band at 841 cm^{-1} decreases likely due to the appearance of the melting-recrystallization or an increase on the amount of short helix at 973 cm^{-1} which are supposed to be generated from the random coil in amorphous region. The relative change of regularity bands at 841 and 998 cm^{-1} during stepwise heating (Fig. 5c) depicts that the ratio of band intensities at 841 and 998 cm^{-1} increases linearly all along in the whole process, demonstrating a significant growth of long helix at 841 cm^{-1} due to the extension of short helix at

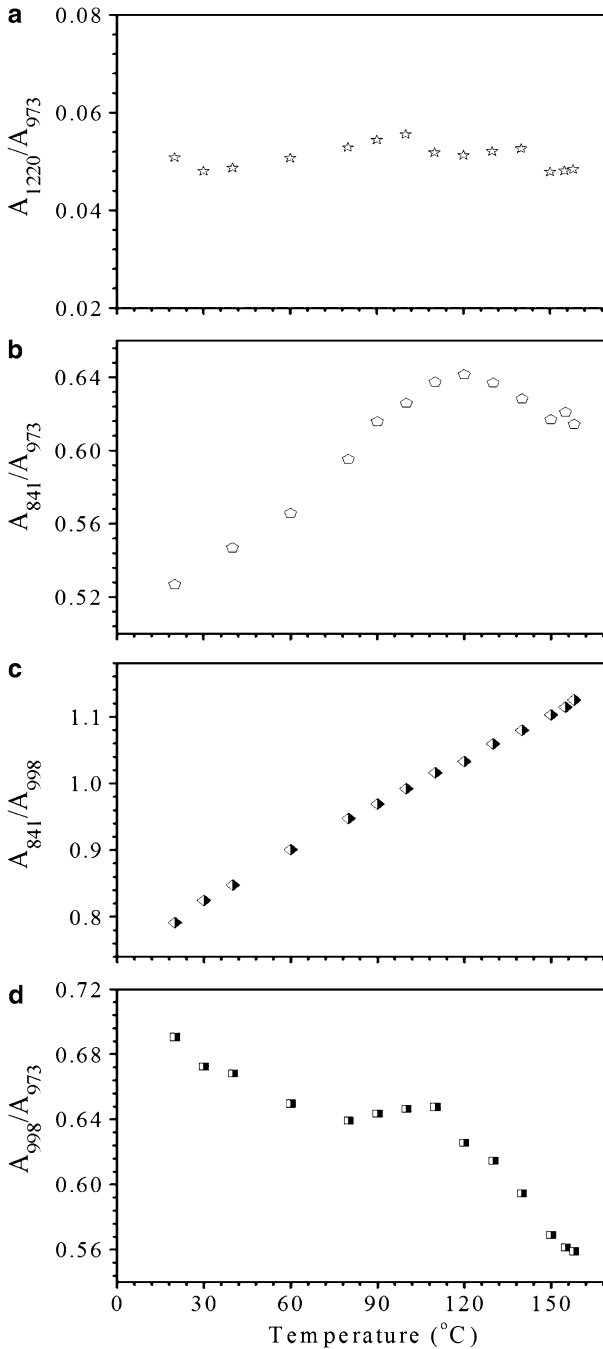


Fig. 5 The plot of intensity ratios of different regularity bands versus temperature from 20 to 158 °C: **a** $A_{1220} \text{ cm}^{-1}/A_{973} \text{ cm}^{-1}$, **b** $A_{841} \text{ cm}^{-1}/A_{973} \text{ cm}^{-1}$, **c** $A_{841} \text{ cm}^{-1}/A_{998} \text{ cm}^{-1}$, and **d** $A_{998} \text{ cm}^{-1}/A_{973} \text{ cm}^{-1}$

998 cm^{-1} . However, the relative change of regularity bands at 998 and 973 cm^{-1} during stepwise heating (Fig. 5d) exhibits that with temperature increasing, the ratio of band intensities at 998 and 973 cm^{-1} first decreases, then remains constant, and subsequently decreases again, which shows the easy growth for the 998 cm^{-1} band to long helix at 841 cm^{-1} compared with the 973 cm^{-1} band.

Combining the results shown in Figs. 4 and 5, it is reasonable to conclude that during heating, for the short helix at 973 cm^{-1} band, on one hand, the increase of the content can be realized by the generation from the random coil in amorphous region. On the other hand, the decrease of the content is due to the extension to the long helix at 841 cm^{-1} . For the regular band at 998 cm^{-1} , probably only the extension to the long helix at 841 cm^{-1} happens. As for the regular band at 841 cm^{-1} , the increase of the content is at the expense of the extension of the regular bands at 973 and 998 cm^{-1} . And the decrease of the content is ascribed to the possible appearance of melting-recrystallization. While for the regular band at 1220 cm^{-1} , no detectable extension of short helix into 1220 cm^{-1} appears during heating. In short, the temperature-induced changes of structure of initially quenched mesomorphic iPP are such a case. For the regular bands at 973, 998, 841, and 1220 cm^{-1} , we can affirm that the shortest helix at 973 cm^{-1} can be produced from the random coil in amorphous region. And the growth of 998 cm^{-1} band to long regularity band at 841 cm^{-1} is quite easier than that of the 973 cm^{-1} band. At the same time, the limited increment of the higher order regularity band at 1220 cm^{-1} is found.

From Figs. 4 and 5, one can also be seen that the mechanism of extension of short helix into long one is dominant when the temperature is lower than 120 °C, and then possible melting-recrystallization for the higher order regularity band occurs as the temperature is higher than 120 °C. Obviously, a structure change occurs in the vicinity of 120 °C. It is consistent with the results of previous literatures [3, 16, 29–31] reported.

In summary, changes of structure of initially quenched mesomorphic iPP during stepwise heating investigated in this study can give us new insights on the mesomorphic-to-monoclinic phase transition mechanism. That is to say, the mesomorphic-to-monoclinic phase transition undergoes melting-recrystallization, and the extension of short helix into long one but with the limited enhancement of ordering, which can be as a proof and supplement to the previous phase transition mechanisms outlined in [18, 31].

Conclusions

Heat-induced conformational changes of quenched mesomorphic iPP are monitored through analyzing the variation of the regularity bands by in situ FT-IR spectroscopy. The experimental results show that the mechanism of extension of short helix into long one is dominant before 120 °C, and then possible melting-recrystallization for the higher order regularity band occurs after 120 °C. Furthermore, it is easier for 998 cm^{-1} band to extend into long one than that of 973 cm^{-1} band. And the content of higher order regularity band at 1220 cm^{-1}

remains almost invariable during stepwise heating, which shows the limited increment of higher order regularity band. In a word, all these changes of structure of initially quenched mesomorphic iPP induced by temperature may give us new insights on the mesomorphic-to-monoclinic phase transition mechanism in some sense.

Acknowledgments The authors acknowledge the financial support from the National Natural Science Foundation of China (20804051) and Natural Science Foundation of Hebei Province (B2010001055). The authors also appreciate the much helpful comments from the reviewers.

References

1. Natta G, Corradini P (1960) Structure and properties of isotactic polypropylene. *Nuovo Cimento (Suppl)* 15:40–51
2. Natta G, Peraldo M, Corradini P (1959) Smectic mesomorphic form of isotactic polypropylene. *Rend Accad Naz Lincei* 26:14–17
3. Hsu CC, Geil PH, Miyaji H, Asai K (1960) Structure and properties of polypropylene crystallized from the glassy state. *J Polym Sci Polym Phys* 24:2379–2401
4. Wunderlich B, Gerbowicz J (1984) Thermotropic mesophases and mesophase transitions of linear, flexible macromolecules. *Adv Polym Sci* 60(61):1–59
5. Grebowicz J, Lau S-F, Wunderlich B (1984) The thermal properties of polypropylene. *J Polym Sci Polym Symp* 71:19–37
6. Mcallister PB, Carter TJ, Hinde RM (1978) Structure of the quenched form of polypropylene. *J Polym Sci Polym Phys* 16:49–57
7. Miller RL (1960) On the existence of near-range order in isotactic polypropylenes. *Polymer* 1:135–143
8. Gailey JA, Ralston RH (1964) The quenched state of polypropylene. *SPE Trans* 4:29–33
9. Bodor G, Grell M, Kallo A (1964) Untersuchung des zustandes von polypropylen-vorschlag zur bestimmung der kristallinität des polypropylens. *Faserforsch Textiltech* 15:527–532
10. Corradini P, Petraccone V, De Rosa C, Guerra G (1986) On the structure of the quenched mesomorphic phase of isotactic polypropylene. *Macromolecules* 19:2699–2703
11. Androsch R, Di Lorenzo ML, Schick C, Wunderlich B (2010) Mesophases in polyethylene, polypropylene, and poly(1-butene). *Polymer* 51:4639–4662
12. Zia Q, Radosch HJ, Androsch R (2009) Deformation behavior of isotactic polypropylene crystallized via a mesophase. *Polym Bull* 63:755–771
13. Singh G, Kaur S, Kothari AV, Naik DG, Vyas PB, Gupta VK (2009) Studies on the influence of molecular weight and isotacticity of polypropylene on the formation of mesomorphic phase. *J Appl Polym Sci* 113:3181–3186
14. Koch T, Seidler S, Halwax E, Bernstorff S (2007) Microhardness of quenched and annealed isotactic polypropylene. *J Mater Sci* 42:5318–5326
15. Mileva D, Androsch R, Zhuravlev E, Schick C (2009) Temperature of melting of the mesophase of isotactic polypropylene. *Macromolecules* 42:7275–7278
16. Zia Q, Androsch R, Radosch HJ, Piccarolo S (2006) Morphology, reorganization and stability of mesomorphic nanocrystals in isotactic polypropylene. *Polymer* 47:8163–8172
17. Zia Q, Androsch R, Radosch HJ, Ingolic E (2008) Crystal morphology of rapidly cooled isotactic polypropylene: a comparative study by TEM and AFM. *Polym Bull* 60:791–798
18. Wang ZG, Hsiao BS, Srinivas S, Brown GM, Tsou AH, Cheng SZD, Stein RS (2001) Phase transformation in quenched mesomorphic isotactic polypropylene. *Polymer* 42:7561–7566
19. Androsch R (2008) In situ atomic force microscopy of the mesomorphic-monoclinic phase transition in isotactic polypropylene. *Macromolecules* 41:533–535
20. Marega C, Causin V, Marigo A (2008) A SAXS–WAXD study on the mesomorphic- α transition of isotactic polypropylene. *J Appl Polym Sci* 109:32–37

21. Arvidson SA, Khan SA, Gorga RE (2010) Mesomorphic- α -monoclinic phase transition in isotactic polypropylene: a study of processing effects on structure and mechanical properties. *Macromolecules* 43:2916–2924
22. Konishi T, Nishida K, Kanaya T (2006) Crystallization of isotactic polypropylene from prequenched mesomorphic phase. *Macromolecules* 39:8035–8040
23. Li B, Li L, Zhao L, Yuan WK (2008) In situ FT-IR spectroscopic study on the conformational changes of isotactic polypropylene in the presence of supercritical CO₂. *Eur Polym J* 44:2619–2624
24. Zhu XY, Yan DY, Yao HX, Zhu PF (2000) In situ FTIR spectroscopic study of the regularity bands and partial-order melts of isotactic poly(propylene). *Macromol Rapid Commun* 21:354–357
25. Kissin YV (1974) Structures of copolymers of high olefins. *Adv Polym Sci* 15:91–155
26. Hanna LA, Hendra PJ, Maddams W, Willis HA, Zichy V, Cudby MEA (1988) Vibrational spectroscopic study of structural changes in isotactic polypropylene below the melting point. *Polymer* 29:1843–1847
27. Passingham C, Hendra PJ, Cudby MEA, Zichy V, Weller M (1990) The re-evaluation of multiple peaks in the DSC melting endotherm of isotactic polypropylene. *Eur Polym J* 26:631–638
28. Kissin YV, Rishina LA (1976) Regularity bands in the i.r. spectra of C₃H₆–C₃D₆ copolymers. *Eur Polym J* 12:757–759
29. Zia Q, Radosch HJ, Androsch R (2007) Direct analysis of annealing of nodular crystals in isotactic polypropylene by atomic force microscopy, and its correlation with calorimetric data. *Polymer* 48:3504–3511
30. Grubb DT, Yoon DY (1986) Morphology of quenched and annealed isotactic polypropylene. *Polym Commun* 27:84–88
31. Zhao JC, Qiu J, Niu YH, Wang ZG (2009) Evolutions of morphology and crystalline ordering upon annealing of quenched isotactic polypropylene. *J Polym Sci Polym Phys* 47:1703–1712